Enhancement of Notch receptor maturation and signaling sensitivity by Cripto-1

Kazuhide Watanabe,[1] Tadahiro Nagaoka,[1] Joseph M. Lee,[1] Caterina Bianco,[1] Monica Gonzales,[1] Nadia P. Castro,[1] Maria Cristina Rangel,[1] Kei Sakamoto,[2] Youping Sun,[3] Robert Callahan,[1] and David S. Salomon[1]

[1]Mammary Biology and Tumorigenesis Laboratory, Center for Cancer Research, National Cancer Institute, National Institutes of Health, Bethesda, MD 20892
[2]Oral Pathology, Tokyo Medical and Dental University Graduate School, Bunkyo-ku, Tokyo 113-8549, Japan
[3]Department of Cell Biology, Harvard Medical School, Boston, MA 02115

Nodal and Notch signaling pathways play essential roles in vertebrate development. Through a yeast two-hybrid screening, we identified Notch3 as a candidate binding partner of the Nodal coreceptor Cripto-1. Coimmunoprecipitation analysis confirmed the binding of Cripto-1 with all four mammalian Notch receptors. Deletion analyses revealed that the binding of Cripto-1 and Notch1 is mediated by the Cripto-1/FRL-1/Cryptic domain of Cripto-1 and the C-terminal region of epidermal growth factor–like repeats of Notch1. Binding of Cripto-1 to Notch1 occurred mainly in the endoplasmic reticulum–Golgi network. Cripto-1 expression resulted in the recruitment of Notch1 protein into lipid raft microdomains and enhancement of the furin-like protein convertase-mediated proteolytic maturation of Notch1 (S1 cleavage). Enhanced S1 cleavage resulted in the sensitization to ligand-induced activation of Notch signaling. In addition, knockdown of Cripto-1 expression in human and mouse embryonal carcinoma cells desensitized the ligand-induced Notch signaling activation. These results suggest a novel role of Cripto-1 in facilitating the post-translational maturation of Notch receptors.

Introduction

The Nodal and Notch signaling pathways perform crucial roles in regulating various stages of embryonic development (Bolós et al., 2007; Shen, 2007). Nodal is a member of the TGF-β family; its signaling activity is required to establish the anterior–posterior and the left–right body axes and to determine cell lineages for the initiation of gastrulation (Shen, 2007). Nodal utilizes a shared Smad2/3-dependent signaling pathway with other TGF-β family ligands such as activin or TGF-β. Unlike other TGF-β family ligands, Nodal requires glycosylphosphatidylinositol-anchored coreceptors, EGF–Cripto-1/FRL-1/Cryptic (CFC) family proteins which include human and mouse Cripto-1 (CR-1/Cr-1) and Cryptic (CFC1), for activation of Alk4/ActRIIB receptor signaling (Strizzi et al., 2005).

Notch signaling regulates a variety of developmental processes, including asymmetric cell division, left–right asymmetry, somitogenesis, and development of various types of organ systems such as the central nervous and cardiovascular systems (Bolós et al., 2007). Mammals have four Notch receptors (Notch1–4) and five membrane-bound ligands (Dll1, -3, and -4 and Jagged-1 and -2). Mature Notch receptors are expressed as heteromeric single-pass transmembrane proteins after proteolytic maturation by furin-like protein convertase (S1 cleavage). Ligand binding induces sequential cleavage of Notch receptors at the extracellular domain (ECD) by ADAM (a disintegrin and metalloprotease) proteinase (S2 cleavage) and at the transmembrane domain by a γ-secretase enzyme complex (S3 cleavage), releasing an intracellular domain (ICD). The Notch ICD then translocates to the nucleus, where it associates with the DNA-binding protein CBF1 (CSL/RBPJ-κ) to regulate the transcription of multiple effecter genes, including members of the HES/HEY family (Bolós et al., 2007).

In this study, we discovered an unexpected function of EGF-CFC proteins in the Notch signaling pathway. Our findings provide a new insight into Notch and Nodal/CR-1 signaling pathways.

Correspondence to Kazuhide Watanabe: kazuhidew@yahoo.com; or David S. Salomon: salomond@mail.nih.gov

Abbreviations used in this paper: BFA, brefeldin A; CFC, Cripto-1/FRL-1/Cryptic; EC, embryonal carcinoma; ECD, extracellular domain; FL, full length; GAPDH, glyceraldehyde 3-phosphate dehydrogenase; ICD, intracellular domain; IP, immunoprecipitation; PE, phycoerythrin; SA, streptavidin; WT, wild type; Y2H, yeast two-hybrid.

The Rockefeller University Press $30.00
J. Cell Biol. Vol. 187 No. 3 343–353
www.jcb.org/cgi/doi/10.1083/jcb.200905105

Results and discussion

It has been suggested that EGF-CFC proteins function independently of Nodal in vertebrate development (Warga and Kane, 2003; D'Andrea et al., 2008). Therefore, we assumed that there may exist unknown binding partners of CR-1. To discover novel binding partners of CR-1, we used a yeast two-hybrid (Y2H) screening approach. A core peptide sequence of human CR-1 (aa 34–161) was used as a bait to screen a mouse embryo or human colon cDNA prey library for potential binding partners. A prey encoding mouse Notch3 (aa 1,290–1,478) was isolated from the screening after passage through two auxotrophic reporters. Five additional candidate genes were also isolated through this screening procedure (Table I). Two of six candidate proteins comprised secreted or cell-associated extracellular proteins, EFEMP2 and Notch3, both of which contain large EGF-like repeats. To confirm the interaction between CR-1 and Notch3 in a mammalian expression system, coimmunoprecipitation (co-IP) assays were performed using Flag-tagged CR-1 (CR-Flag) and HA-tagged full-length (FL) Notch3 (N3FL-HA) in transiently transfected COS-7 cells (Fig. 1 C). N3FL-HA was pulled down by anti-Flag antibody only in the presence of CR-Flag, and, vice versa, CR-Flag was pulled down by anti-HA antibody only in the presence of N3FL-HA. We also detected similar interactions of CR-1 with other Notch receptors (Notch1, -2, and -4; Fig. 1, A, B, and D, respectively). These interactions were observed with other cell lines such as CHO or 293T cells, suggesting that the binding of CR-1 to Notch is not cell type specific (unpublished data). CR-1 preferentially bound to the FL Notch precursors (~300 kD) but not to the cleaved forms (120 kD). To detect the interaction of endogenous proteins, we used NTERA2/D1 human embryonal carcinoma (EC) cells, which express high levels of CR-1 as well as Notch receptors (Fig. 1 E; Ciccodicola et al., 1989; Walsh and Andrews, 2003). We used two polyclonal antibodies, C20 and AF5317, which recognize the ICD and ECD of Notch1, respectively, for Notch IP. Both antibodies coimmunoprecipitated endogenous CR-1 protein (Fig. 1 F). Reciprocally, the ~300-kD forms of endogenous Notch1 and -2 were pulled down with the endogenous CR-1 protein (Fig. 1 G). We also confirmed the binding of endogenous mouse Cr-1 and Notch1 proteins in F9 mouse EC cells (Fig. S1 A). In addition to CR-1, the other member of the EGF-CFC family, CFC1, was also able to bind to the Notch1 protein (Fig. 1 H).

We then attempted to identify the binding domains within CR-1 and the Notch receptors using a series of deletion mutants (Fig. 2, A and B). Whereas a deletion of the EGF-like domain of CR-1 (ΔEGF) still retained its binding affinity for Notch1, deletion of the CFC domain (ΔCFC) diminished the ability of CR-1 to interact with Notch1 (Fig. 2 C). Deletion of both the EGF-like and CFC domains (ΔEΔC) was required to completely abolish the interaction with Notch1 (Fig. 2 C). This suggested that the CFC domain of CR-1 is primarily responsible for mediating the binding to Notch1. We also performed deletion experiments with the Notch1 protein (Fig. 2, D–F). Deletion of all three Lin12 repeats (ΔLNR) of Notch1 did not affect the Notch1–CR-1 interaction (Fig. 2 D), suggesting that the EGF-like repeats of Notch1 are responsible for the Notch1–CR-1 binding. To test whether binding of CR-1 is specific for the EGF-like repeats of Notch receptors, we replaced all of the EGF-like repeats with EGF-like repeats of a Notch ligand Dll1 (DlEGF + NΔEGF and DlEGF + NΔECD). DlEGF + NΔEGF and DlEGF + NΔECD failed to interact with CR-1 (Fig. 2 D). CR-1 also did not bind to FL Dll1 (Fig. 2 E). These data suggest that CR-1 binding is specific to the EGF-like repeats of Notch1. Constructs containing up to the first six EGF-like repeats of Notch1 (2×, 4×, and 6× EGF) were not sufficient to efficiently bind CR-1 (Fig. 2 D). Similarly, the Notch1 ICD did not show any binding to CR-1 (Fig. 2 D), confirming that the interaction between CR-1 and Notch1 is mediated by the ECD of Notch1. To further identify the precise location of the CR-1–interacting EGF-like repeats in Notch1, we generated deletion constructs lacking EGF-like repeats 8–24 (ΔEGF8–24 and ΔMfeI), a region which is essential for ligand binding (Ge et al., 2008). These two constructs were able to bind to CR-1 with an affinity similar to FL Notch1, suggesting that the binding of Notch1 to CR-1 is independent of the ligand-binding domain of Notch1 (Fig. 2 E). To pinpoint the EGF-like repeats responsible for CR-1 binding, we generated artificial constructs containing seven of the C-terminal EGF-like repeats (N1EGF30-YFP), the last two EGF-like repeats (N1EGF35-YFP), or only the LNR (N1LNR-YFP). Co-IP assays revealed that the binding of N1EGF30- and N1EGF35-YFP to CR-1 was comparable with the positive control N2FL-Myc, but the binding to CR-1 was dramatically reduced with N1LNR-YFP (Fig. 2 F). This suggests that the last two EGF-like repeats are necessary and sufficient for CR-1 binding. This result is in agreement with the region in Notch3 that was detected by the Y2H screen because this prey fragment

Table I. **Candidate binding partners of CR-1 from Y2H screening**

Bait	Bait aa coordinates	Prey	Gene ID	Prey aa coordinates	Library
Human TDGF1	34–161	AHNAK	79026	5,648–5,891	Human colon
Human TDGF1	34–161	mCDH4[a]	107932	1,591–1,865 1,591–1,903 1,590–1,720	Mouse embryo
Human TDGF1	34–161	mEFEMP2	58859	256–440	Mouse embryo
Human TDGF1	34–161	mHUWE1	59026	3,494–3,736	Mouse embryo
Human TDGF1	34–161	mPLSCR3	70310	19–297	Mouse embryo
Human TDGF1	34–161	mNotch3	18131	1,290–1,478	Mouse embryo

Gene identification (ID) numbers are from the Entrez Gene database.

[a]Three independent clones were identified.

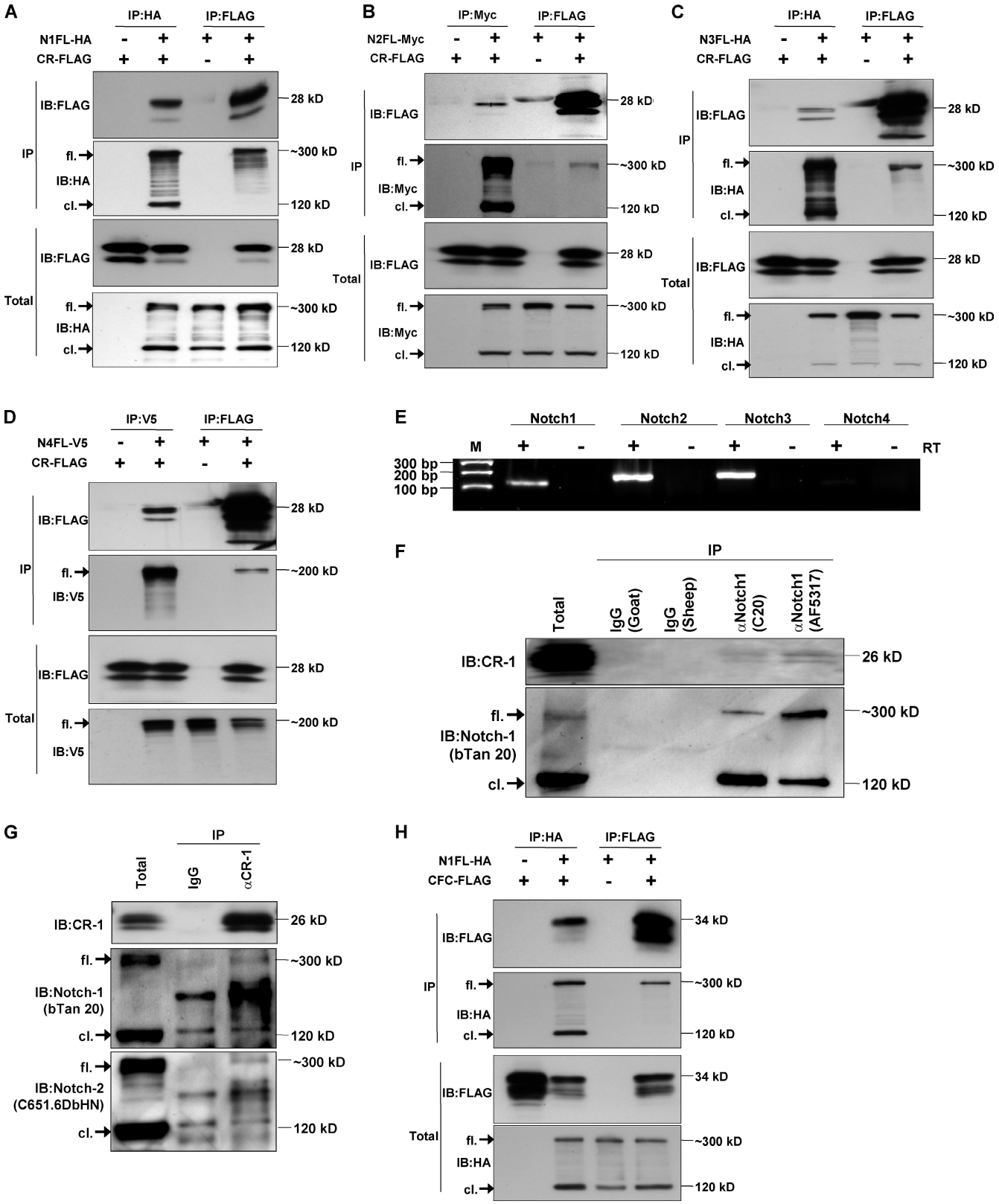

Figure 1. **CR-1 physically associates with all four Notch receptors.** (A–D) Flag-tagged CR-1 (CR-Flag) was cotransfected with HA-tagged Notch1 (N1FL-HA; A), Myc-tagged Notch2 (N2FL-Myc; B), HA-tagged Notch3 (N3FL-HA; C), and V5-tagged Notch4 (N4FL-V5; D) in COS-7 cells. IP and immunoblotting (IB) were performed with the indicated antibodies. cl., cleaved Notch proteins; fl., FL Notch proteins. (E) Nonquantitative RT-PCR for Notch receptor expression in NTERA2/D1 cells. M, markers. (F and G) Interaction between endogenous CR-1 and Notch1/2 in NTERA2/D1 cells. (F) Notch1 IP was performed using anti-Notch1 polyclonal antibodies (C20 and AF5317). (G) CR-1 IP was performed with anti–CR-1 goat polyclonal antibody (α–CR-1). Normal goat or sheep IgGs were used as negative controls. Proteins were detected with the indicated antibodies. (H) Flag-tagged CFC1 (CFC-Flag) was cotransfected with N1FL-HA, and co-IP was performed as described in A–D.

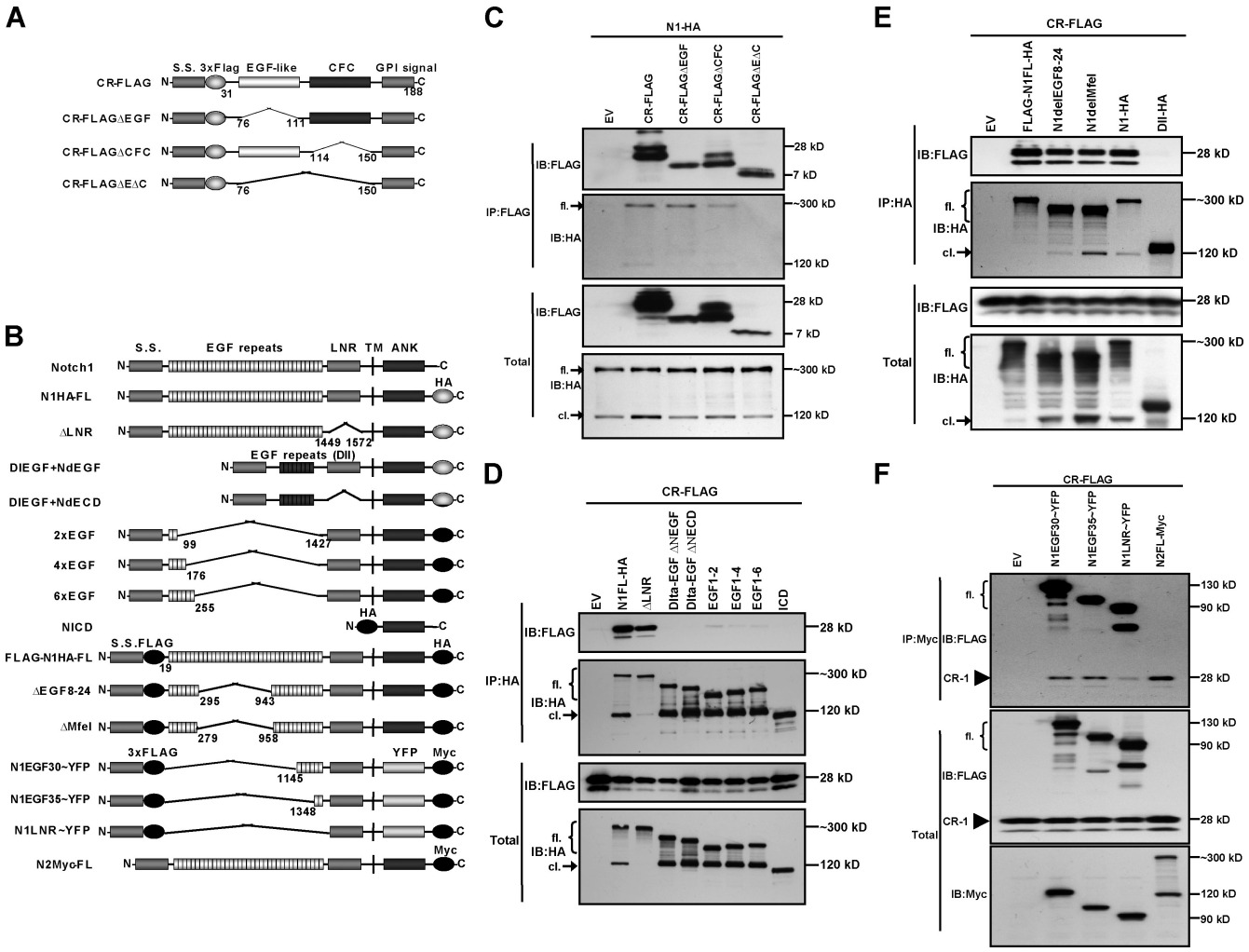

Figure 2. **Deletion analysis of the CR-1–Notch interaction.** (A) CR-1 deletions. (B) Notch1 deletions/chimeras. (C–F) Co-IP was performed using anti-Flag (C), anti-HA (D and E), or anti-Myc (F) affinity beads. Proteins were detected with the indicated antibodies. cl., cleaved Notch proteins; EV, empty vector; fl., FL Notch proteins; IB, immunoblot; S.S., signal sequence.

(aa 1,290–1,478) contained the last two EGF-like repeats (EGF33 and -34) and LNR 1 and 2 domains of Notch3. Moreover, we also demonstrated that Notch3 binds to CR-1 through the ECD (Fig. S1, B–D). A Notch3 mutant (R1031C), which causes a CADASIL (cerebral autosomal dominant arteriopathy with subcortical infarcts and leukoencephalopathy), did not affect the interaction between CR-1 and Notch3 (Fig. S1, B–D).

To ascertain whether CR-1 binding to Notch1 occurs on the cell surface, we performed a surface biotinylation assay followed by co-IP (Fig. 3 A). We were able to distinguish biotinylated CR-1 protein by an SDS-PAGE mobility shift because each PEG_4-biotin molecule has an ∼0.5-kD molecular mass and the native CR-1 protein is relatively small (∼28 kD). When the biotinylated sample was precipitated with streptavidin (SA) beads, biotinylated as well as unbiotinylated CR-1 were pulled down. This suggests that the unbiotinylated form of CR-1 is bound to other cell surface biotinylated protein or proteins. In fact, when the sample was sequentially precipitated with anti-Flag and SA beads, only the biotinylated form of CR-1 was precipitated. Biotinylated Notch1 was indistinguishable by size because the Notch1 molecule has a large molecular mass (∼300 kD). A 120-kD form of Notch was enriched in SA-precipitated samples as described previously (Bush et al., 2001). We did not observe any detectable cell surface binding of Notch1 to CR-1 in the sequentially immunoprecipitated sample. These data suggest that CR-1 binding to Notch1 occurs mainly within the cell, even though we cannot entirely exclude the possibility of any cell surface interaction between Notch1 and CR-1, which might be below the limit of detection by this assay method. In addition, the binding of CR-1 to Notch1 interaction was independent of glycosylation because treatment with tunicamycin did not affect this binding (Fig. 3 B). The mobility shift of CR-1 and of the FL form of Notch1 confirmed that both proteins underwent protein glycosylation. Confocal analysis of GFP-labeled CR-1 and HA-tagged Notch1 (N1FL-HA) revealed that both proteins showed a typical perinuclear vesicular pattern, suggesting an ER/Golgi localization (Fig. 3 C and Fig. S2, A and B). Analysis with higher magnification revealed that these two proteins can colocalize mainly in the same intracellular vesicles. Finally, brefeldin A (BFA) treatment, which interferes with Golgi to membrane trafficking and almost completely blocks cell surface expression of CR-1 (Fig. 3 D), did not

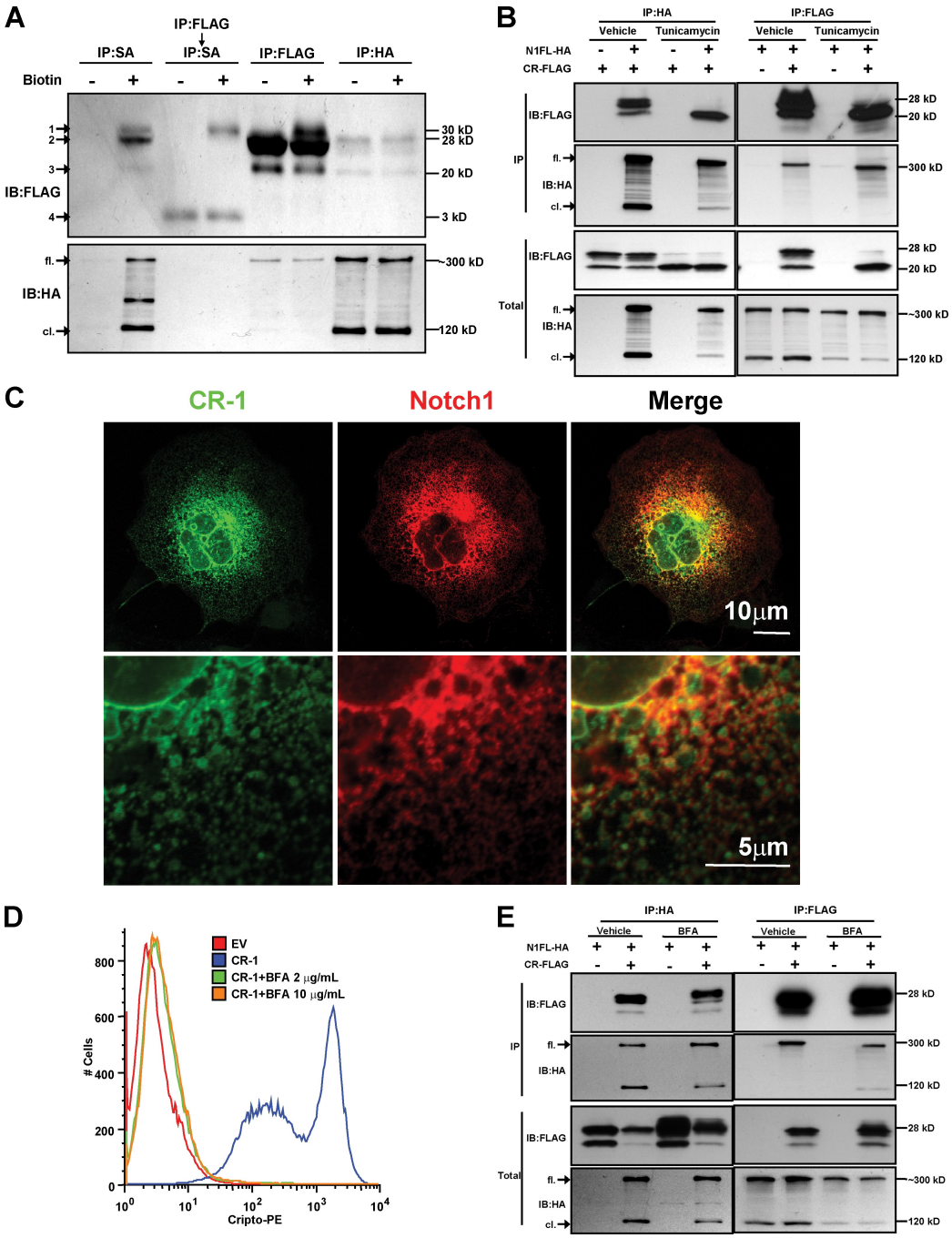

Figure 3. **Intracellular interaction of CR-1 and Notch1.** (A) Cell surface biotinylation assay. Transiently transfected COS-7 cells were treated with *N*-hydroxysuccinimide–PEG_4-biotin. Co-IP or sequential co-IP was performed with the indicated antibodies. Each indicated band corresponds as follows: 1, biotinylated CR-1; 2, unbiotinylated and glycosylated CR-1; 3, unbiotinylated and unglycosylated CR-1; 4, carryover of 3× Flag peptides used for Flag elution. (B) Effect of glycosylation on the CR-1–Notch1 interaction. COS-7 cells were treated with vehicle or 10 μg/ml tunicamycin for 16 h after transient transfection. Co-IP assays were performed reciprocally. (C) Intracellular localization of CR-1 and Notch1. GFP-tagged CR-1 and N1FL-HA were visualized by a confocal microscope. (D) Cell surface expression of CR-1 after BFA treatment. Transiently transfected COS-7 cells were treated with the indicated concentrations of BFA for 16 h. Cells were stained with PE-conjugated anti–CR-1 mAb, and FACS analysis was performed. (E) Transiently transfected COS-7 cells were treated with vehicle or 2 μg/ml BFA for 16 h, and the co-IP experiment was performed using the indicated antibodies. cl., cleaved Notch proteins; fl., FL Notch proteins; IB, immunoblot.

affect the binding of CR-1 to Notch1 (Fig. 3 E). These results suggest that the binding between CR-1 and Notch1 may occur inside the cell and possibly before or during protein processing in the ER/Golgi complex.

To assess whether the binding of CR-1 to Notch1 may affect Notch signaling, we used a CBF1-dependent Notch reporter assay system (TP-1 reporter) after ligand stimulation in a co-culture assay (Fig. 4 A). When CHO cells transfected with the TP-1 reporter were stimulated by co-culture with wild-type (WT) or ligand-expressing L cells (L-WT, L-Dll1, or L–Jagged-1), the signal enhancement by these ligands was subtle but detectable (Fig. 4 A). However, when the FL Notch1 (N1FL) was

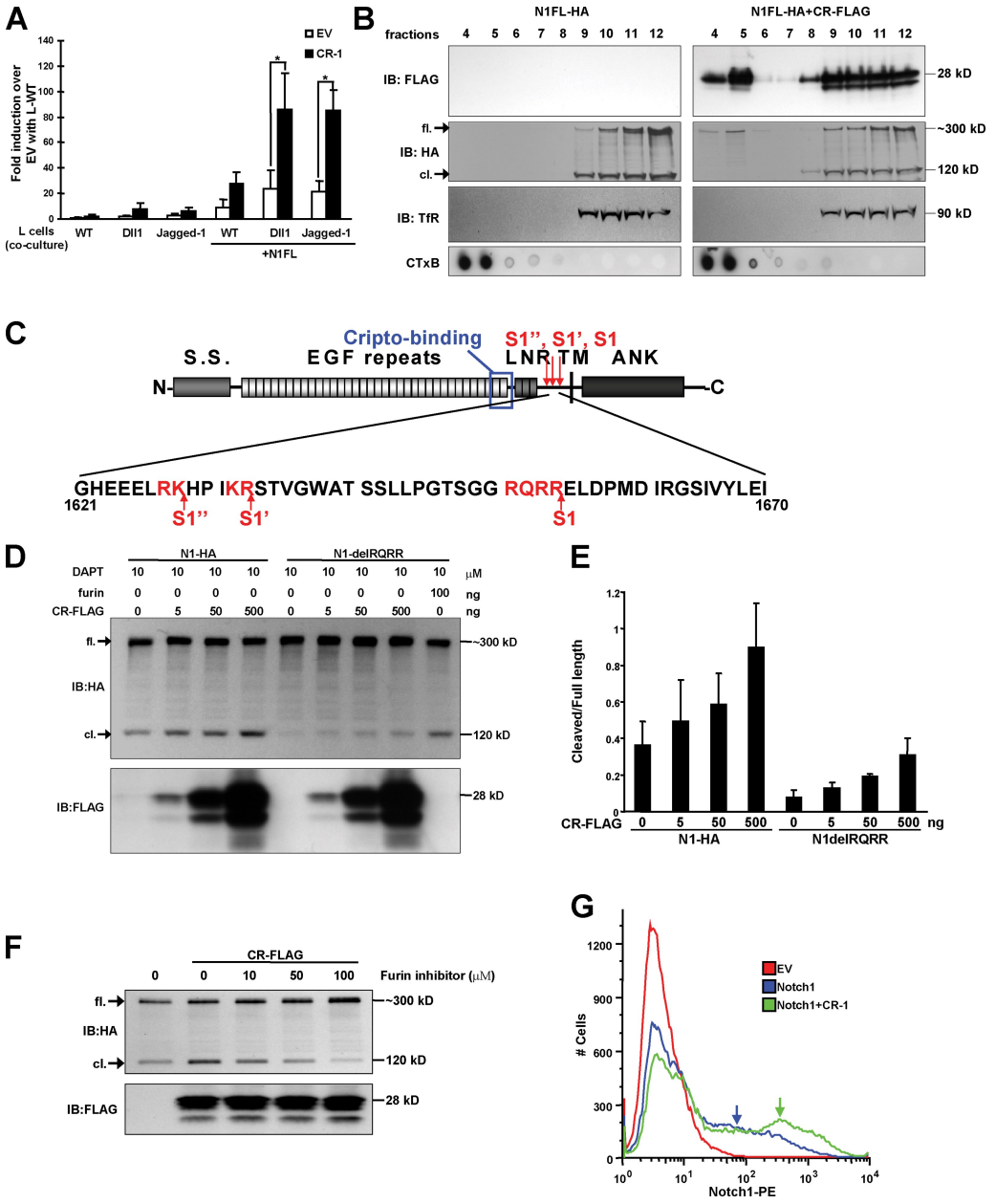

Figure 4. **Sensitization of the Notch signaling pathway by CR-1.** (A) TP-1 reporter assay of co-cultured CHO cells with L-WT, L-Dll1, or L–Jagged-1 cells. CHO cells were transiently transfected with empty vector (EV) or WT CR-1 expression vector before co-culture. Cotransfection of FL Notch1 (N1FL) was also performed. Mean ± SD is shown for three independent experiments. *, $P < 0.05$. (B) Sucrose gradient isolation of lipid rafts in transiently transfected CHO cells. Fractions 4–5 correspond to the lipid raft fractions. Transferrin receptor (TfR) or Cholera toxin B (CTxB) was used as a nonraft or lipid raft marker, respectively. IB, immunoblot. (C) S1 cleavage sites of Notch1. ANK, ankyrin domain; S.S., signal sequence; TM, transmembrane domain. (D and E) Enhancement of S1 cleavage of Notch1 by CR-1 expression. CHO cells transiently transfected with the indicated amount of expression vectors were incubated with 10 μM DAPT for 24 h and analyzed by Western blotting. Mean ± SD of densitometric quantification is shown for three independent transfections (E). (F) Blockade of CR-1–induced Notch processing by a furin inhibitor. Transiently transfected CHO cells were treated with the indicated concentrations of a furin inhibitor, Decanoyl-RVKR-chloromethylketone, for 24 h, and Notch processing was analyzed as described in D. (G) Enhanced cell surface expression of Notch1 by CR-1. CHO cells were transfected with the indicated expression vectors, and the cell surface expression level of Notch1 was assessed by FACS analysis. Arrows indicate the peaks of Notch1-transfected populations.

coexpressed, the ligand-induced TP-1 reporter activity was strongly potentiated. Ectopic expression of CR-1 significantly enhanced this ligand-induced TP-1 reporter activation. This effect of CR-1 was not observed with exogenous soluble CR-1 protein (Fig. S2 C).

A recent study has shown that Cr-1 controls processing of the Nodal proprotein by recruiting proprotein convertases such as furin or PACE4 (Blanchet et al., 2008). Because processing by furin-like convertases (S1 cleavage) is also a prerequisite to generate mature heterodimerized Notch receptors (Logeat et al., 1998), we hypothesized that CR-1 may affect this processing step. Similar to the sequestration of the Nodal precursor protein into lipid rafts (Blanchet et al., 2008), forced expression of CR-1 in CR-1–deficient CHO cells enhanced the localization

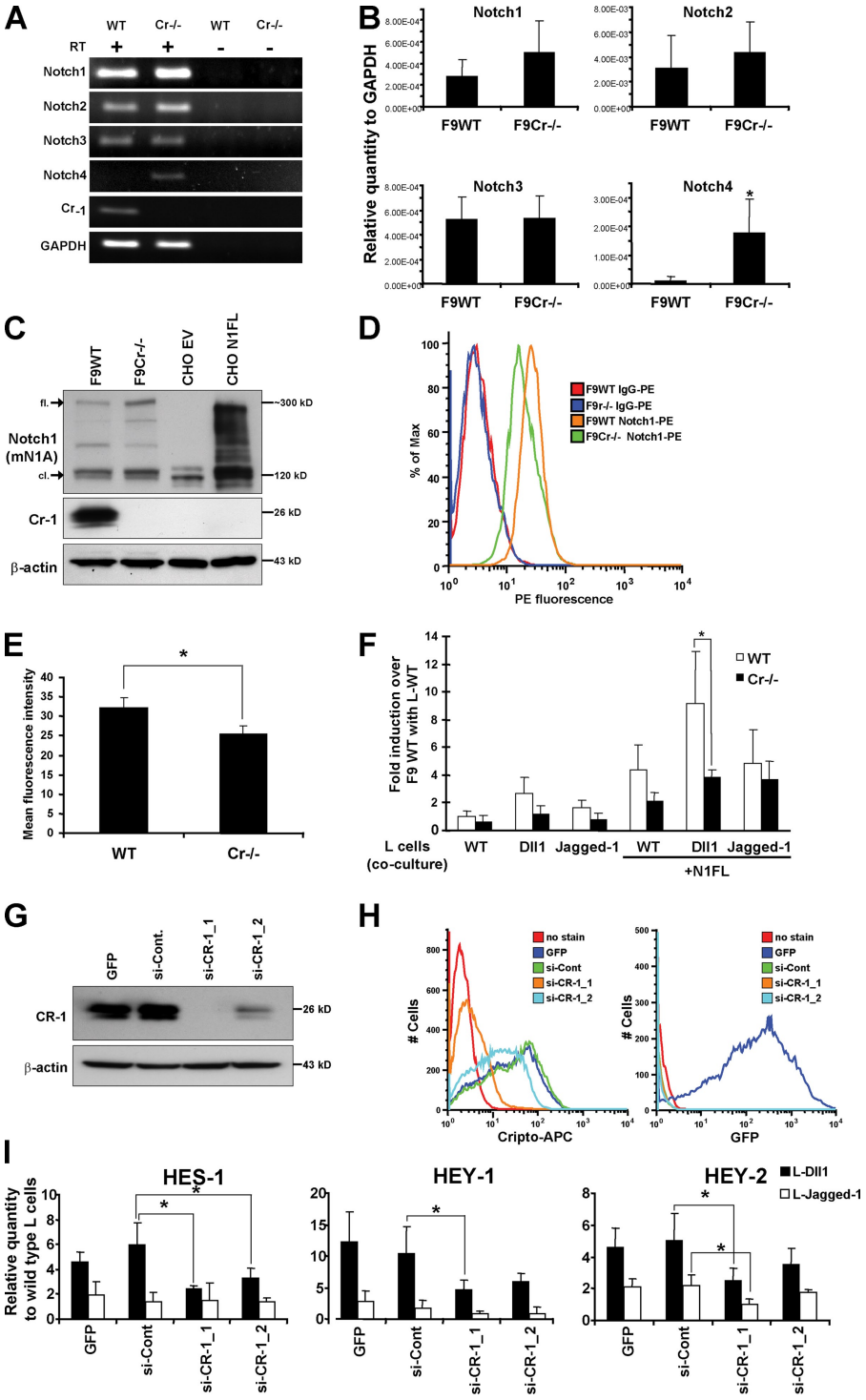

Figure 5. **Functional interaction between endogenous CR-1 and Notch1 in EC cells.** (A–C) Endogenous expression of CR-1 and Notch receptors in F9 WT and $Cr^{-/-}$ cells. (A) Non-quantitative RT-PCR. Samples treated without reverse transcription (RT−) were used as negative controls. (B) Quantitative RT-PCR. Mean ± SD is shown for four independent cultures. *, $P < 0.05$ compared with F9 WT. (C) Western blot analysis. Empty vector– and N1FL-transfected CHO cells (CHO EV and N1FL) were used as negative and positive controls, respectively. cl., cleaved Notch proteins; fl., FL Notch proteins. (D and E) FACS analysis for the cell surface expression of endogenous Notch1 in F9 cells. Mean ± SD is shown for three independent cultures (E). *, $P = 0.021$. (F) Effect of Cr-1 knockdown on ligand-induced TP-1 reporter activity in F9 cells. Transiently transfected F9 WT or $Cr^{-/-}$ cells were co-cultured with L-WT, L-Dll1, or L–Jagged-1 cells. Cotransfection of N1FL was also performed. Mean ± SD of relative values of relative luciferase units is shown for four independent experiments. *, $P < 0.05$. (G and H) siRNA knockdown of CR-1 in NTERA2/D1 cells. Suppression of CR-1 protein by siCR-1_1 and siCR-1_2 was evaluated by Western blotting (G) and FACS analysis (H, left). GFP was used as an indicator of transfection efficiency (>95%; H, right). (I) Effect of CR-1 knockdown on ligand-induced Notch target gene expression in NTERA2/D1 cells. siRNA-transfected NTERA2/D1 cells were co-cultured with L-WT, L–Dll1, or L–Jagged-1 cells. Human Notch target gene expression was assessed by quantitative RT-PCR. Mean ± SD of relative values is shown for four independent experiments. *, $P < 0.05$.

of the FL Notch1 protein in the lipid raft fraction in which glycosylphosphatidylinositol-anchored proteins such as CR-1 are enriched (Fig. 4 B). Furthermore, we assessed the effect of CR-1 expression on S1 cleavage of Notch1 in the presence of the γ-secretase inhibitor DAPT to exclude the effect on ligand-induced S3 cleavage (Fig. 4, C and D). CR-1 expression caused a dose-dependent increase in enhancement of the cleaved form of Notch1. This cleavage enhancement could also be demonstrated with a Notch1 mutant (N1-ΔRQRR) in which one of the furin cleavage sites was deleted (Fig. 4 C; Logeat et al., 1998) but to a much lesser extent (Fig. 4, D and E). The enhanced cleavage of Notch1 by CR-1 is mediated by furin-like convertase because the treatment with a furin inhibitor (Decanoyl-RVKR-chloromethylketone) dose-dependently inhibited the cleavage of Notch1 protein (Fig. 4 F). In addition, we have demonstrated that coexpression of CR-1 increased the cell surface expression of Notch1 as demonstrated for Nodal (Blanchet et al., 2008), suggesting that CR-1 may have a role for membrane trafficking as well as proteolytic maturation of Notch receptors (Fig. 4 G).

To address the biological significance of our findings in a physiological setting, we used mouse and human EC cells in which both Cr-1/CR-1 and Notch proteins are endogenously expressed (Figs. 1 E and 5, A–C and G). F9 mouse EC cells express Cr-1 and several Notch receptors, as detected by RT-PCR and Western blot analysis (Fig. 5, A–C). We obtained a Cr-1–null variant ($Cr^{-/-}$) of F9 cells, which was generated by gene targeting. We confirmed that the endogenous expression of Cr-1 was absent in F9 $Cr^{-/-}$ cells (Fig. 5, A and C). Notch1, -2, and -3 receptors were equally expressed in F9 WT and $Cr^{-/-}$ cells (Fig. 5, A and B). F9 WT cells showed little expression of Notch4, which, in contrast, was detected in $Cr^{-/-}$ cells (Fig. 5, A and B). Western blotting for endogenous Notch1 revealed the expression of the 300-kD precursor form and the 120-kD mature form of Notch1 in F9 WT and $Cr^{-/-}$ cells (Fig. 5 C). However, there was a reduced expression of the 300-kD form in F9 WT cells, as compared with F9 $Cr^{-/-}$ cells, suggesting an enhancement of Notch1 processing by the presence of Cr-1. In fact, the cell surface expression level of Notch1 is higher in F9 WT cells compared with $Cr^{-/-}$ cells (Fig. 5, D and E). Ligand-induced activation of the TP-1 reporter was reduced in F9 $Cr^{-/-}$ cells, as compared with F9 WT cells, and the difference was enhanced when ectopic N1FL was expressed (Fig. 5 F). Like F9 WT cells, NTERA2/D1 human EC cells, from which human CR-1 was originally cloned (Ciccodicola et al., 1989) expressed Notch1, -2, and -3 but not Notch4 (Fig. 1 E). We used siRNAs to knock down endogenous CR-1 expression in NTERA2/D1 cells. We designed two siRNAs, of which siCR-1_1 showed almost a complete knockdown and siCR-1_2 showed an ∼70% knockdown efficiency of the CR-1 protein (Fig. 5, G and H). We performed a co-culture assay of siRNA-transfected NTERA2/D1 cells with L-WT, L-Dll1, or L–Jagged-1 cells to assess the effect of siRNA-mediated knockdown of CR-1 on ligand-induced Notch target gene expression using quantitative RT-PCR with human-specific primer sets that do not cross-react with mouse cDNAs from L cells (Fig. S3). As shown in Fig. 5 I, CR-1 knockdown in NTERA2/D1 cells significantly suppressed to varying degrees the induction of the Notch target genes (HES-1 and HEY-1 and -2) after Notch ligand stimulation.

In this study, we discovered a novel mechanism for sensitization of the Notch signaling pathway by CR-1 through the direct binding to the intracellular pro form of the Notch receptors. Finally, the mechanism by which CR-1 facilitates Notch receptor signaling is by the enhancement of S1 cleavage through a furin-like convertase. In fact, the CR-1–binding domain of Notch1 is proximal to the S1 cleavage sites (Fig. 4 C). This processing step is essential for the cell surface expression of Notch receptors and for ligand-induced activation of the Notch receptors, at least in mammals (Nichols et al., 2007). The enhanced proteolytic processing of Notch is initiated by CR-1 in intracellular ER/Golgi vesicles that are being exocytosed. This seems likely because binding of CR-1 to Notch could not be detected on the cell surface and because blockade of glycosylation or Golgi to membrane trafficking was unable to perturb binding. We also demonstrated a role of endogenous CR-1/Cr-1 in potentiating the Notch signaling pathway in EC cells.

Both Notch and Nodal/CR-1 signaling pathways are essential for maintenance of stem/progenitor cell populations and for controlling lineage specification (Strizzi et al., 2005; Bolós et al., 2007). In addition, these signaling pathways are involved in the progression of tumors in various types of cancer (Bianco et al., 2005; Bolós et al., 2009). Therefore, our findings have a potential impact on delineating the mechanism by which Notch and Nodal/CR-1 signaling pathways may regulate embryogenesis and carcinogenesis.

Materials and methods

Cell lines

COS-7, CHO, 293T, and NTERA2/D1 cells were purchased from American Type Culture Collection. F9 WT and $Cr^{-/-}$ cells were provided by M. Sanicola (Biogen Idec, Cambridge, MA). L-WT, L-Dll1, and L–Jagged-1 cells were provided by P. Stanley (Albert Einstein College of Medicine, Bronx, NY). Transfections were performed using Lipofectamine 2000 (Invitrogen) for COS-7, CHO, 293T, and F9 cells or using Nucleofector (Lonza) for NTERA2/D1 cells according to the manufacturers' instructions.

Y2H screening

Automated Y2H screening was performed at Myriad Genetics as previously described (Garrus et al., 2001). A bait plasmid coding human CR-1 (aa 34–161) fused to the C terminus of the Gal4 DNA–binding domain (aa 1–147) was transformed into yeast strain PNY200 (*MAT-α ura3-52 ade2-101 trp1-901 his3-Δ200 leu2-3, 112 gal4Δgal80Δ*). Prey constructs were generated from double poly(A)-selected mRNA of mouse embryo or of human colon. The prey constructs were transformed into the yeast strain BK100 (*MATa ura3-52 ade2-101 trp1-901 his3-Δ200 leu2-3, 112 gal4Δgal80ΔGAL2-ADE2 LYS2::GAL1-HIS3 met2::GAL7-lacZ*). PNY200 cells (bait) were mated with BK100 cells (prey). Resulting diploid yeast cells were then selected in the presence of 3 mM 3-amino-1, 2, 4-triazole for the ability to synthesize tryptophan (bait), leucine (prey), histidine (bait–prey interaction), and adenine (bait–prey interaction).

Expression plasmids

All CR-1–, CFC1-, and Notch2-derived constructs were based on human sequences, whereas all Notch1-, Notch3-, and Notch4-related vectors were based on mouse sequences. WT CR-1, CR-Flag, and CFC-Flag expression vectors were described previously (Watanabe et al., 2008). CR-1 deletions (ΔEGF, ΔCFC, and ΔEGFΔCFC) were generated by PCR-based methods. GFP fusion CR-1 constructs were cloned into the pCI-neo expression vector (Promega). N1FL-HA, ΔLNR, DlEGF + NΔEGF, DlEGF + NΔECD, 2–6× EGF, N1ICD, and Dll-HA were previously described (Sakamoto et al., 2002, 2005). N1ΔEGF8–24 was generated by a PCR-based method with the Flag-N1-HA expression vector as a template. NΔMfeI is a self-ligated product after MfeI digestion of the Flag-N1-HA vector. N1EGF30-, N1EGF35-, and N1LNR-YFP were generated by PCR and cloned into the p3× Flag–Myc-CMV-24 expression vector (Sigma-Aldrich). WT N1FL was a gift from R. Kopan (Washington University in St. Louis, St. Louis, MO). The N1-ΔRQRR mutant construct was generated by mutagenesis. N2FL-Myc, N3FL-HA, R1031C mutant Notch3 from a CADASIL patient (N3FLmt-HA), N3ICD-HA, N3ECD-Myc, and TP-1 reporter were provided by S. Artavanis-Tsakonas (Harvard University, Cambridge, MA). N4FL-V5 was generated by introducing mouse Notch4 cDNA (gift from Y. Shirayoshi, Tottori University, Tottori, Japan) into the EcoRI–NotI site of the pEF6/V5-His TOPO TA expression vector (Invitrogen). This construct is C-terminally truncated at an intrinsic NotI site (truncation of aa 1,890–1,964). DsRed-Golgi and a mouse furin expression vector were purchased from Takara Bio Inc. and Thermo Fisher Scientific, respectively. All primer sequences used for vector construction are provided in Table II.

IP, sequential IP, and Western blot analysis

Whole cell lysates were prepared using IP buffer (2 mM Na orthovanadate, 50 mM NaF, 20 mM Hepes, 150 mM NaCl, 1.5 mM $MgCl_2$, 5 mM Na pyrophosphate, 10% glycerol, and 0.2% Triton X-100). IP was performed using anti–Flag M2, anti-HA, anti-V5, anti-Myc affinity gel (Sigma-Aldrich), or SA agarose (Invitrogen). Sequential IP was performed by eluting the Flag-precipitated proteins with 3× Flag peptide followed by a second IP. Proteins were separated on 4–20% SDS-PAGE gels (Invitrogen). Epitope tags were detected with peroxidase conjugates of anti–Flag M2, anti-Myc (Sigma-Aldrich), anti-HA (Roche), and anti-V5 (Invitrogen) antibodies. Endogenous human CR-1 and mouse Cr-1 were detected with B3F6 mAb

Table II. **Oligonucleotide DNA/RNAs used in this study**

Name	Sequence	Description	Product size
Primers for CR-1 mutants			
CR-1–F-NotI	5′-GCGGCCGCGCTGGGCCATCAGGAA-3′	Forward	
CR-1ΔEGF-F	5′-CCATGGGGATACAGCACAGTAAAGAGAACTGTGGGTCTGT-3′	Deletion	
CR-1ΔEGF-R	5′-ACAGACCCACAGTTCTCTTTACTGTGCTGTATCCCCATGG-3′	Deletion	
CR-1ΔCFC-F	5′-AGCACGATGTGCGCAAAGAGGGCCTTGTGATGGATGAGCA-3′	Deletion	
CR-1ΔCFC-R	5′-TGCTCATCCATCACAAGGCCCTCTTTGCGCACATCGTGCT-3′	Deletion	
CR-1ΔEΔC-F	5′-CCCATGGGGATACAGCACAGTGGCCTTGTGATGGATGAGCAC-3′	Deletion	
CR-1ΔEΔC-R	5′-GTGCTCATCCATCACAAGGCCACTGTGCTGTATCCCCATGGG-3′	Deletion	
CR-1–R-EcoRI	5′-GAATTCTTAATAGTAGCTTTGTATAGA-3′	Reverse	
Primers for Notch1 mutants			
N1Mfel-F	5′-CAATTGCCGCTGCCCACCGGA-3′	Forward	
N1ΔEGF8–24-F	5′-GGACGGGTCAGTACTGTACAGAGGACATCAATGAATGTG-3′	Deletion	
N1ΔEGF8–24-R	5′-GCACATTCATTGATGTCCTCTGTACAGTACTGACCCGTC-3′	Deletion	
N1Mfel-R	5′-CAATTGGCACCATTTTGGCAG-3′	Reverse	
N1EGF30-F-EcoRI	5′-GAATTCAGAGGTGGACGAGTGCTCACCT-3′	Forward	
N1EGF35-F-EcoRI	5′-GAATTCAGATGCCCGCACTTGTGGCAGC-3′	Forward	
N1LNR-F-EcoRI	5′-GAATTCAGAGCTGCCTGAGTGCCAGGTG-3′	Chimeric	
N1-YFP-F	5′-CGCAAGCGCCGGCGGCAGCATGTGAGCAAGGGCGAGGAGCTG-3′	Chimeric	
N1-YFP-R	5′-CAGCTCCTCGCCCTTGCTCACATGCTGCCGCCGGCGCTTGCG-3′	Chimeric	
YFP-R-XbaI	5′-TCTAGACTTGTACAGCTCGTCCATGCC-3′	Reverse	
N1-ΔRQRR-F	5′-GTACCAGTGGTGGGGAGCTGGACCCCAT-3′	Mutagenesis	
N1-ΔRQRR-R	5′-ATGGGGTCCAGCTCCCCACCACTGGTAC-3′	Mutagenesis	
PCR primers[a]			
mNotch1-F	5′-ACAACAACGAGTGTGAGTCC-3′		221 bp
mNotch1-R	5′-ACACGTGGCTCCTGTATATG-3′		221 bp
mNotch2-F	5′-TGACTGTTCCCTCACTATGG-3′		150 bp
mNotch2-R	5′-CACGTCTTGCTATTCCTCTG-3′		150 bp
mNotch3-F	5′-AGATCAATGAGTGTGCATCC-3′		158 bp
mNotch3-R	5′-GCAGACTCCATGACTACAGG-3′		158 bp
mNotch4-F	5′-CTCTTGCCACTCAATTTCCCT-3′		188 bp
mNotch4-R	5′-TTGCAGAGTTGGGTATCCCTG-3′		188 bp
hNotch1-F	5′-AGGACCTCATCAACTCACACGC-3′		130 bp
hNotch1-R	5′-TCTTTGTTAGCCCCGTTCTTCAG-3′		130 bp
hNotch2-F	5′-CCGTGTTGACTTCTGCTCTCTCAC-3′		170 bp
hNotch2-R	5′-CCTACTACCCTTGGCATCCTTTG-3′		170 bp
hNotch3-F	5′-TCTCAGACTGGTCCGAATCCAC-3′		171 bp
hNotch3-R	5′-ACACTTGCCTCTTGGGGGTAAC-3′		171 bp
hNotch4-F	5′-ATGCGAGGAAGATACGGAGTGG-3′		112 bp
hNotch4-R	5′-TCGGAATGTTGGAGGCAGAAC-3′		112 bp
hHes-1–F[b]	5′-AGGCGGACATTCTGGAAATG-3′		103 bp
hHes-1–R[b]	5′-CGGTACTTCCCCAGCACACTT-3′		103 bp
hHey-1–F[b]	5′-GAAACTTGAGTTCGGCTCTAGG-3′		113 bp
hHey-1–R[b]	5′-GCTTAGCAGATCCTTGCTCCAT-3′		113 bp
hHey-2–F[b]	5′-GGCGTCGGGATCGGATAAATA-3′		127 bp
hHey-2–R[b]	5′-AAGTAGCCTTTACCCCCTGTT-3′		127 bp
hGAPDH-F[b]	5′-GGACCTGACCTGCCGTCTAGAA-3′		141 bp
hGAPDH-R[b]	5′-GGTGTCGCTGTTGAAGTCAGAG-3′		141 bp
mCr-1–F	5′-ATGGACGCAACTGTGAACATGATGTTCGCA-3′		174 bp
mCr-1–R	5′-CTTTGAGGTCCTGGTCCATCACGTGACCAT-3′		174 bp
mHes-1–F[c]	5′-TCCTAACGCAGTGTCACCTTCCAG-3′		148 bp
mHes-1–R[c]	5′-CCAAGTTCGTTTTTAGTGTCCGTC-3′		148 bp
mHey-1–F[c]	5′-CAGGAGGGAAAGGTTATTTTGACG-3′		163 bp
mHey-1–R[c]	5′-TAGTTGTTGAGATGGGAGACCAGGCG-3′		163 bp
mGAPDH-F[c]	5′-AATGTGTCCGTCGTGGATCT-3′		256 bp
mGAPDH-R[c]	5′-CCCTGTTGCTGTAGCCGTAT-3′		256 bp
siRNAs			
siCR-1_1-S	5′-CGCUUCUCUUACAGUGUGA-3′		
siCR-1_1-AS	5′-UCACACUGUAAGAGAAGCG-3′		
siCR-1_2-S	5′-GAAUUAUAUGUUCAGAUUA-3′		
siCR-1_2-AS	5′-UAAUCUGAACAUAUAAUUC-3′		

Blank cells indicate that the information is not applicable.

[a]Used for both quantitative PCR and conventional RT-PCR; [b]Human specific (no cross-reactivity with mouse cDNA); [c]Mouse specific (no cross-reactivity with human cDNA).

(Biogen Idec) and with anti–mouse Cr-1 rabbit polyclonal antibody (Cell Signaling Technology), respectively. Human Notch1 and -2 and mouse Notch1 proteins were detected with rat Notch1 mAb (bTan 20; Developmental Studies Hybridoma Bank), rat Notch2 mAb (C651.6DbHN; Developmental Studies Hybridoma Bank), and mouse Notch1 mAb (mN1A; Santa Cruz Biotechnology, Inc.), respectively. Endogenous CR-1 and human and mouse Notch1 proteins were immunoprecipitated with anti–CR-1 goat polyclonal antibody (V17; Santa Cruz Biotechnology, Inc.), anti–human Notch1 polyclonal antibodies (C20 [Santa Cruz Biotechnology, Inc.] and AF5317 [R&D Systems]), and mouse Notch1 mAb (mN1A). Densitometric quantification of band intensity was performed using Labworks software (UVP, Inc.).

Cell surface biotinylation
24 h after transfection, 2×10^7 cells were washed with PBS, pH 8.0, four times and incubated with 2 mM *N*-hydroxysuccinimide–PEG_4-biotin (Thermo Fisher Scientific) for 30 min on ice. The reaction was quenched by washing with PBS containing 100 mM glycine.

Immunofluorescence
Transiently transfected COS-7 cells were fixed in 4% PFA and permeabilized with 0.2% Triton X-100. After blocking with PBS containing 10% BSA and 10% normal goat serum, samples were incubated with anti-HA antibody (Covance) for 1 h at RT. Primary antibody was then labeled with Alexa Fluor 596–conjugated secondary antibody (Invitrogen). Counterstaining for nuclei was performed with DAPI, and samples were mounted with ProLong Gold antifade reagent (Invitrogen). Images were taken at RT with a confocal system (LSM 710 NLO; Carl Zeiss, Inc.) with an inverted microscope (Axiovert 200M; Carl Zeiss, Inc.) equipped with a 63× NA 1.4 Plan-Apochromat oil immersion objective lens. Images were collected with AIM software (Carl Zeiss, Inc.) using a multitrack configuration.

FACS analysis
As described previously (Watanabe et al., 2007b), cells were collected with enzyme-free cell dissociation buffer (PBS containing 4 mM EDTA). After washing with ice-cold FACS buffer (PBS with 0.1% BSA), 1.0×10^5 cells were incubated for 20 min with anti–human CR-1 phycoerythrin (PE)-conjugated antibody (FAB2772P; R&D Systems) at a dilution of 1:50 or PE-conjugated anti-Notch1 mAb (BioLegend). Cells were then pelleted, resuspended in 500 µl of ice-cold FACS buffer, and analyzed using a FACScan instrument (BD).

Sucrose gradient isolation of lipid rafts
As described previously (Watanabe et al., 2007a), cells were washed with cold PBS, scraped into 2 ml MBS (2-[*N*-morpholino] ethanesulfonic acid–buffered saline, 25 mM 2-[*N*-morpholino] ethanesulfonic acid, pH 6.5, and 0.15 M NaCl) containing 1% Triton X-100, and solubilized for 20 min at 4°C. After homogenization by 10 strokes with a tight-fitting homogenizer (Dounce; Wheaton Science Products), samples were adjusted to 40% sucrose by the addition of 2 ml of 80% sucrose. Then, a 5–40% discontinuous sucrose gradient was formed and centrifuged at 40,000 rpm for 20 h in an SW40Ti rotor (Beckman Coulter). 12 1-ml fractions were removed from the top of the tubes and analyzed by Western and dot blotting.

Dual luciferase assay
Dual luciferase assay using a co-culture system with ligand-expressing L cells was performed as previously described with slight modifications (Stahl et al., 2008). CHO or F9 cells were plated in 24-well culture plates (5×10^5 cells/well) and were transiently transfected with TP-1 reporter, TK-renilla, and an N1FL and/or a CR-Flag expression vector. 16 h after transfection, L cells were plated onto the CHO or F9 cells (5×10^6 cells/well) and incubated for 30 h. Dual luciferase assays (Promega) were performed according to manufacturer's instructions.

RNA extraction and RT-PCR
Total RNA was extracted using the RNA mini kit (QIAGEN). On-column DNase treatment was performed for all RNA extractions. cDNA was prepared from 1 µg of total RNA using the Retroscript kit (Applied Biosystems). All nonquantitative PCR described in this study was performed at 25 cycles of 94°C (30 s), 55°C (30 s), and 72°C (30 s) using the PCR master mix (QIAGEN). Quantitative PCR was performed using an MX3000P PCR and Brilliant SYBR green QPCR master mix (Agilent Technologies). Comparative analyses were performed between the genes of interest and the housekeeping gene *glyceraldehyde 3-phosphate dehydrogenase* (*GAPDH*). All forward and reverse PCR primer sequences are provided in Table II.

siRNA treatment
Sequences for siCR-1_1 and siCR-1_2 are provided in Table II. Control siRNA targeting firefly luciferase mRNA was purchased from Thermo Fisher Scientific. Lonza nucleofections were performed with 2×10^6 subconfluent NTERA2/D1 cells in the L kit (Lonza) containing 1 µM of each siRNA or 0.5 µg of GFP control vector and plated into 6-well plates. After 16 h of nucleofection, 5×10^6 L cells were seeded onto a sheet of NTERA2/D1 cells and incubated for 30 h. RNA extraction and quantitative RT-PCR were performed as described in the previous section.

Statistical analysis
Two-tailed Student's *t* test was used to determine the statistical significance of the quantitative results. Results with a p-value <0.05 were considered statistically significant.

Online supplemental material
Fig. S1 shows a co-IP assay of Cr-1 and Notch1 in F9 cells and a deletion analysis of Notch3 proteins for binding to CR-1. Fig. S2 shows colocalization of CR-1 and Notch1 proteins with a Golgi marker and the effect of soluble CR-1 on Notch signaling activity. Fig. S3 shows the amplification plots of quantitative RT-PCR confirming the specificity of human- or mouse-specific primers used in this study. Online supplemental material is available at http://www.jcb.org/cgi/content/full/jcb.200905105/DC1.

We are grateful to Drs. Michele Sanicola, Pamela Stanley, Raphael Kopan, Spyros Artavanis-Tsakonas, Joseph Arboleda-Velasquez (Harvard Medical School, Boston, MA), and Yasuaki Shirayoshi for providing reagents.

This work was supported by National Institutes of Health intramural funding.

Submitted: 19 May 2009
Accepted: 5 October 2009

References

Bianco, C., L. Strizzi, N. Normanno, N. Khan, and D.S. Salomon. 2005. Cripto-1: an oncofetal gene with many faces. *Curr. Top. Dev. Biol.* 67:85–133. doi:10.1016/S0070-2153(05)67003-2

Blanchet, M.H., J.A. Le Good, D. Mesnard, V. Oorschot, S. Baflast, G. Minchiotti, J. Klumperman, and D.B. Constam. 2008. Cripto recruits Furin and PACE4 and controls Nodal trafficking during proteolytic maturation. *EMBO J.* 27:2580–2591. doi:10.1038/emboj.2008.174

Bolós, V., J. Grego-Bessa, and J.L. de la Pompa. 2007. Notch signaling in development and cancer. *Endocr. Rev.* 28:339–363. doi:10.1210/er.2006-0046

Bolós, V., M. Blanco, V. Medina, G. Aparicio, S. Díaz-Prado, and E. Grande. 2009. Notch signalling in cancer stem cells. *Clin. Transl. Oncol.* 11: 11–19. doi:10.1007/s12094-009-0305-2

Bush, G., G. diSibio, A. Miyamoto, J.B. Denault, R. Leduc, and G. Weinmaster. 2001. Ligand-induced signaling in the absence of furin processing of Notch1. *Dev. Biol.* 229:494–502. doi:10.1006/dbio.2000.9992

Ciccodicola, A., R. Dono, S. Obici, A. Simeone, M. Zollo, and M.G. Persico. 1989. Molecular characterization of a gene of the 'EGF family' expressed in undifferentiated human NTERA2 teratocarcinoma cells. *EMBO J.* 8:1987–1991.

D'Andrea, D., G.L. Liguori, J.A. Le Good, E. Lonardo, O. Andersson, D.B. Constam, M.G. Persico, and G. Minchiotti. 2008. Cripto promotes A–P axis specification independently of its stimulatory effect on Nodal autoinduction. *J. Cell Biol.* 180:597–605. doi:10.1083/jcb.200709090

Garrus, J.E., U.K. von Schwedler, O.W. Pornillos, S.G. Morham, K.H. Zavitz, H.E. Wang, D.A. Wettstein, K.M. Stray, M. Côté, R.L. Rich, et al. 2001. Tsg101 and the vacuolar protein sorting pathway are essential for HIV-1 budding. *Cell*. 107:55–65. doi:10.1016/S0092-8674(01)00506-2

Ge, C., T. Liu, X. Hou, and P. Stanley. 2008. In vivo consequences of deleting EGF repeats 8-12 including the ligand binding domain of mouse Notch1. *BMC Dev. Biol.* 8:48. doi:10.1186/1471-213X-8-48

Logeat, F., C. Bessia, C. Brou, O. LeBail, S. Jarriault, N.G. Seidah, and A. Israël. 1998. The Notch1 receptor is cleaved constitutively by a furin-like convertase. *Proc. Natl. Acad. Sci. USA*. 95:8108–8112. doi:10.1073/pnas.95.14.8108

Nichols, J.T., A. Miyamoto, S.L. Olsen, B. D'Souza, C. Yao, and G. Weinmaster. 2007. DSL ligand endocytosis physically dissociates Notch1 heterodimers before activating proteolysis can occur. *J. Cell Biol.* 176:445–458. doi:10.1083/jcb.200609014

Sakamoto, K., O. Ohara, M. Takagi, S. Takeda, and K. Katsube. 2002. Intracellular cell-autonomous association of Notch and its ligands: a novel mechanism

of Notch signal modification. *Dev. Biol.* 241:313–326. doi:10.1006/dbio.2001.0517

Sakamoto, K., W.S. Chao, K. Katsube, and A. Yamaguchi. 2005. Distinct roles of EGF repeats for the Notch signaling system. *Exp. Cell Res.* 302:281–291. doi:10.1016/j.yexcr.2004.09.016

Shen, M.M. 2007. Nodal signaling: developmental roles and regulation. *Development*. 134:1023–1034. doi:10.1242/dev.000166

Stahl, M., K. Uemura, C. Ge, S. Shi, Y. Tashima, and P. Stanley. 2008. Roles of Pofut1 and O-fucose in mammalian Notch signaling. *J. Biol. Chem.* 283:13638–13651. doi:10.1074/jbc.M802027200

Strizzi, L., C. Bianco, N. Normanno, and D. Salomon. 2005. Cripto-1: a multifunctional modulator during embryogenesis and oncogenesis. *Oncogene*. 24:5731–5741. doi:10.1038/sj.onc.1208918

Walsh, J., and P.W. Andrews. 2003. Expression of Wnt and Notch pathway genes in a pluripotent human embryonal carcinoma cell line and embryonic stem cell. *APMIS*. 111:197–210, discussion :210–211. doi:10.1034/j.1600-0463.2003.1110124.x

Warga, R.M., and D.A. Kane. 2003. One-eyed pinhead regulates cell motility independent of Squint/Cyclops signaling. *Dev. Biol.* 261:391–411. doi:10.1016/S0012-1606(03)00328-2

Watanabe, K., C. Bianco, L. Strizzi, S. Hamada, M. Mancino, V. Bailly, W. Mo, D. Wen, K. Miatkowski, M. Gonzales, et al. 2007a. Growth factor induction of Cripto-1 shedding by glycosylphosphatidylinositol-phospholipase D and enhancement of endothelial cell migration. *J. Biol. Chem.* 282:31643–31655. doi:10.1074/jbc.M702713200

Watanabe, K., S. Hamada, C. Bianco, M. Mancino, T. Nagaoka, M. Gonzales, V. Bailly, L. Strizzi, and D.S. Salomon. 2007b. Requirement of glycosylphosphatidylinositol anchor of Cripto-1 for trans activity as a Nodal co-receptor. *J. Biol. Chem.* 282:35772–35786. doi:10.1074/jbc.M707351200

Watanabe, K., T. Nagaoka, L. Strizzi, M. Mancino, M. Gonzales, C. Bianco, and D.S. Salomon. 2008. Characterization of the glycosylphosphatidylinositol-anchor signal sequence of human Cryptic with a hydrophilic extension. *Biochim. Biophys. Acta*. 1778:2671–2681. doi:10.1016/j.bbamem.2008.09.011